Evaluation of the Oxidizing Potential of Ru and Ru-Pt/ZrO_2 Catalysts for NO Oxidation in the Presence of C_3H_6 and O_2*

A. M. SERRANO-SÁNCHEZ, P. STELTENPOHL, M. P. GONZÁLEZ-MARCOS, J. A. GONZÁLEZ-MARCOS, and J. R. GONZÁLEZ-VELASCO**

Department of Chemical Engineering, Faculty of Sciences, University of the Basque Country/EHU. P.O. Box 644 – E-48080 Bilbao
e-mail: iqpgovej@lg.ehu.es

Received 1 April 2003

The behaviour of Ru and Ru-Pt catalysts supported by ZrO_2 used for NO oxidation was studied in the presence of C_3H_6 and O_2. A qualitative correlation between physicochemical properties of the catalysts and their activity and selectivity in the NO oxidation is discussed. A high NO oxidation potential of the catalysts was encountered to give NO_2, CO_2, and H_2O as the main products. The observed activity is directly related to the catalyst Ru content as well as to the Ru-Pt interaction. The Ru catalyst prepared by impregnation was the most active and stable even though the reaction was carried out in oxidizing atmosphere. Metal-support (Ru-ZrO_2) and metal-metal (Ru-Pt) interactions were found to be responsible for Ru phase stabilization in the catalysts. Ruthenium enhances oxidation processes, as the highest content of noninteracting ruthenium leads to lower oxidation, for NO, and ignition, for C_3H_6, temperatures. Platinum presence in the catalysts enhances the CO formation which is directly related to the metal-metal interaction.

Besides Pt, Ru has demonstrated excellent ability to reduce different substances, including NO_x [1—4]. On the other hand, its instability and variability of its oxidation state in redox reactions have also been reported [5] highlighting that at temperatures exceeding 800 ℃ formation of volatile RuO_3 and RuO_4 from RuO_2 is probable in oxidizing atmosphere [6, 7].

Volatility of Ru might be suppressed by interactions of ruthenium with support and/or second metallic component under dynamic conditions [8, 9]. *Kobylinski et al.* [9] studied NO_x reduction over Ru/Al_2O_3 doped by BaO reporting negligible loss of Ru for reaction temperatures below 538 ℃ under a 4 vol. % of O_2 in helium stream.

Anyhow, the use of ruthenium in applications requiring high thermal stability, such as three-way catalytic system [10], is doubtful. On the contrary, it is a potential oxidative catalyst in the CRT-particles trap technology for the soot abatement assisted by NO_x in diesel engines, operating at temperatures about 300—350 ℃ and lean conditions with an air to fuel ratio greater than 19 [11, 12].

During the last 20 years an extensive use of ruthenium in electrocatalysis [13] and the problem of highly volatile $Ru(CO)_x$ formation has been forcing scientists to investigate the way to stabilize the ruthenium phase. The most promising possibility seems to be the incorporation of another metallic phase into the catalyst composition, or even supporting Ru onto more suitable solids [4, 5, 14—18].

Platinum has been chosen as the second metal with high catalytic potential. Ru-Pt clusters are formed all over metal composition range showing an acceptable stability in reducing as well as oxidizing conditions. Moreover, both metals are easily reducible and represent a well-defined stoichiometry when H_2 is used for chemisorption experiments [15].

Use of ZrO_2 as catalyst and support has increased in recent years [19]. It was extensively used to prepare superacid catalyst through incorporation of SO_4^{2-} groups into its crystalline structure [20, 21]. As support, it presents good mechanical and thermal resistance and a well-developed surface ensures the suitable dispersion of active phases. Moreover, ZrO_2 is able to develop significant metal-support interactions with Pt and Ru [21—23].

The aim of this work is to evaluate the oxidizing potential of Ru and Ru-Pt/ZrO_2 catalysts, once Ru has been stabilized, and search for qualitative correlation between activity and structural properties, for future application in soot abatement assisted by NO_x. Then, the catalyst behaviour is investigated in oxygen-

*Presented at the 30th International Conference of the Slovak Society of Chemical Engineering, Tatranské Matliare, 26—30 May 2003.

**The author to whom the correspondence should be addressed.

rich conditions for NO oxidation in the presence of C_3H_6 and O_2, *i.e.* the environment typical for the exhaust gas from diesel engines.

EXPERIMENTAL

ZrO_2-Supported Ru catalysts were prepared by the liquid-phase adsorption (A) of ruthenium nitrosyl nitrate onto the support surface, or by its impregnation (I). Details on preparation can be found elsewhere [24]. Bimetallic Ru-Pt catalysts were prepared by co-adsorption (CA) or co-impregnation (CI) of zirconia with ruthenium nitrosyl nitrate and hexachloroplatinic acid.

The support, zirconia (ISA), was supplied by the Norton Company. The oxide was ground and sieved to a particle size ranging from 0.16 mm to 0.25 mm, and calcined at 773 K. Textural properties of zirconia were determined from the nitrogen adsorption isotherms, resulting in the following: specific surface area 63.3 $m^2\ g^{-1}$; average pore diameter 8.60 nm. The ZrO_2 isoelectric point of 6.5 was determined by electrophoresis [25] using a Malvern Instrument Zetasizer 4.

Co-adsorption was carried out at room temperature and atmospheric pressure for 3 h in a continuously stirred vessel, in which ZrO_2 was immersed into a metal salt solution with a solution-to-support ratio of 40 $cm^3\ g^{-1}$. The pH value of Ru and Pt precursor solutions was lower than 3, a value sufficiently low compared to the isoelectric point of zirconia, thus promoting the adsorption of the complex metal anions. Then, the resulting solid (adsorbed and co-adsorbed catalyst precursor) was separated from the solution and washed on a filter.

Co-impregnation was performed at 35 °C in rotavapor with a solution-to-support ratio of 10 $cm^3\ g^{-1}$. Solution and support were stirred at atmospheric pressure for 10 min to ensure that the pores of solid were completely filled with metal salts solution. Then, the pressure was set to 50 mbar to evaporate the solvent, and after drying the co-impregnated catalyst precursor was obtained.

All catalyst precursors were dried at 120 °C for 12 h in N_2. A part of co-adsorbed precursor was calcined in air at 300 °C for 1 h instead of being dried. Then, precursors were reduced in a H_2 stream at 500 °C. D denominates the dried and C the calcined catalyst precursors, *i.e.* AD, ID, CAD, CID, and CAC.

An ARL FISONS 3410 + inductively coupled plasma spectroscopy (ICP) equipment was used to determine the actual metal loading of the catalysts.

TPR of the catalyst precursors was used to determine the presence of metal-metal interaction. Pulse chemisorption of hydrogen was employed to calculate the catalyst dispersion. Both techniques were carried out in an Autochem 2910 Micromeritics apparatus. Before TPR experiments, solids were cleaned by passing a stream of N_2 at 50 °C. TPR data were obtained for the temperature range from −50 to 500 °C in a flow of 5 vol. % of H_2 in Ar, using a thermal conductivity detector (TCD).

Prior to the pulse chemisorption experiment, the catalyst surface was degassed by heating from ambient temperature to 500 °C in Ar. Then, the sample was cooled to 0 °C and hydrogen pulses were injected into the argon stream. The amount of hydrogen adsorbed by the sample was measured by TCD.

The reaction of 1000 vol. ppm of NO with 1000 vol. ppm of C_3H_6 was carried out in the presence of 4.5 vol. % of O_2, and N_2 (balance). The feed stream, regulated by mass flow controllers, was introduced in a tubular reactor. Inside the reactor an 8.1 cm^3 catalytic bed composed of 1 g of the catalyst diluted by quartz was contacted with the gas flowing in a descendant direction. The GHSV was set to 25 000 h^{-1}. Reaction temperature was measured and controlled by a thermocouple positioned in the middle of the catalytic bed. The gas leaving the reactor was cooled, and then aspired by a vacuum pump to force the reactants and/or products to pass through the analyzers, placed between the cooler and the pump.

The analyzers, all from Rosemount, consist of a paramagnetic O_2 analyzer model 755, a chemiluminescence NO and NO_x analyzer model 915A, a FID hydrocarbon analyzer model 400A, and two nondispersive infrared analyzers: one for CO, model 880, and the another of double cell for NH_3 and N_2O, model BINOS 1004.2. All analyzers, as well as the temperature controller, were connected to a digital register ALMEMO 5590-2 V5 from AMR.

Concentrations of N_2, CO_2, and H_2O, as reaction products were calculated according to the atomic mass balance of N, C, and H using the following equations

$$[N_2] = \frac{[NO]_{inlet} - ([NO] + [NO_2] + 2\,[N_2O] + [NH_3])_{outlet}}{2} \quad (1)$$

$$[CO_2] = 3\,([C_3H_6]_{inlet} - [C_3H_6]_{outlet}) - [CO] \quad (2)$$

$$[H_2O] = \frac{6\,([C_3H_6]_{inlet} - [C_3H_6]_{outlet}) - 3\,[NH_3]}{2} \quad (3)$$

Prior reaction, the bed was kept at 450 °C for 8 h, with the aim to stabilize the catalysts activity. After this treatment, reaction was carried out at stationary conditions in the temperature range from 150 °C to 500 °C.

RESULTS AND DISCUSSION

Catalyst Preparation and Characterization

Nominal Ru content of monometallic precursors was 1.0 mass % and 1.8 mass % for adsorbed and impregnated precursors, respectively. Bimetallic precursors contained 1.0 mass % of Ru and 0.3 mass %

Table 1. Precursors and Catalysts Active Metal Content and the Results of Pulse Chemisorption of Hydrogen on Prepared Catalysts

Catalyst	Metal content/mass %				Pulse chemisorption	
	Precursor		Catalyst			
	Ru	Pt	Ru	Pt	$V_c/(\mu\text{mol g}^{-1})$	D/%
ID	1.83	–	1.39	–	23.57	34
AD	0.70	–	0.67	–	11.00	33
CAC	0.70	0.21	0.69	0.20	11.42	31
CAD	0.70	0.21	0.68	0.21	9.66	27
CID	1.00	0.30	0.95	0.28	8.85	18

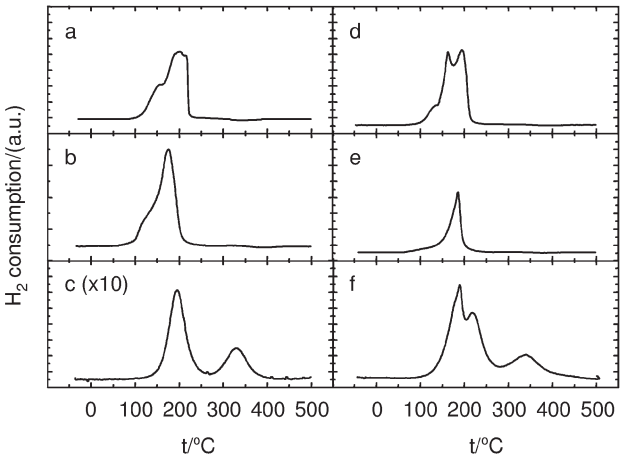

Fig. 1. TPR profiles for monometallic and bimetallic catalyst precursors: *a*) Ru impregnated, *b*) Ru adsorbed, *c*) Pt adsorbed, *d*) Ru-Pt co-impregnated, *e*) Ru-Pt co-adsorbed, *f*) mixture of monometallic Ru adsorbed and Pt adsorbed precursors.

of Pt. The actual metal loading of the corresponding catalyst precursors and catalysts as measured by ICP is shown in Table 1. Results of hydrogen pulse chemisorption and deduced dispersion values considering a H_2/metal ratio of 2 [2, 26] are also shown in Table 1.

During the catalyst activation step, some metal is lost. The difference between the metal content of catalyst precursors and that of corresponding activated catalysts could be, therefore, used as a measure of the stability of supported metal complexes. Meanwhile the metal content of adsorbed (AD) and co-adsorbed (CAD and CAC) precursors and catalysts is very similar; when impregnated (ID) and co-impregnated (CID) precursors and catalysts are compared, the metal loading differs.

Hence, a stronger Ru bond to the support surface was observed for the catalyst prepared by co-adsorption. Moreover, it could be stated that the addition of Pt stabilizes the Ru phase, probably due to their mutual interaction.

In order to prove the presence of interactions between platinum and ruthenium, some TPR experiments were performed. In Fig. 1 (left-hand side) the thermograms obtained for monometallic Pt adsorbed, Ru adsorbed, and Ru impregnated precursors are shown. On the right-hand side, the thermograms of co-adsorbed and co-impregnated bimetallic precursors as well as of a sample prepared by physical mixture of both adsorbed Ru and Pt precursors are displayed.

Two reduction peaks can be observed in Fig. 1*c* for the Pt-adsorbed precursor reduction, while for Ru, either adsorbed or impregnated sample, two overlapped hydrogen consumption peaks were found at lower temperature, compared to the Pt precursor reduction.

A physical mixture of Ru and Pt monometallic adsorbed precursors (Fig. 1*f*) showed signals coincident with those of both metal precursors when analyzed separately, revealing no interactions between the separately adsorbed monometallic particles. For CI precursor (Fig. 1*d*), only one H_2 consumption peak corresponding to Pt species reduction was observed. Moreover, the peaks of Ru and Pt reduction appeared partially overlapped. On the other hand, in the TPR signal obtained for CA precursor (Fig. 1*e*), only one sharp peak is observed, an indication of simultaneous reduction of supported Ru and Pt species.

By comparing the TPR profiles of monometallic precursors with those of bimetallic, the alloying of Ru with Pt was proven for the catalyst prepared by co-adsorption and at least a part of Pt interacted with Ru in co-impregnated catalyst precursor. Therefore, formation of bimetallic clusters is more probable when the catalysts are prepared by co-adsorption compared to the catalysts prepared by co-impregnation [5].

Finally, to discern the magnitude of the metal-metal interaction in bimetallic catalysts, the methylcyclopentane hydrogenolysis was carried out [24], as this reaction may provide information about the structural properties of catalysts. Relatively high extent of methylcyclopentane cracking was observed when unalloyed ruthenium catalysts were used. On the other hand, the addition of Pt to Ru catalysts inhibited the cracking, as platinum is less active metal for deep hydrogenolysis reactions.

Earlier studies revealed that bimetallic Ru-Pt catalysts prepared by co-impregnation of Al_2O_3 and SiO_2 exhibit higher interaction, independently of the metal precursor used for the catalyst preparation [20, 27, 28]. Different preparation methods, *e.g.* co-adsorption [21] or successive impregnation lead to segregation of Ru and Pt metal phases. Therefore, the support nature and its interactions with the metal particles seem to be essential for accommodation of the active phase.

Information about interactions between metals and support can be deduced from the dispersion of catalyst metal particles (Table 1). In the case of monometal-

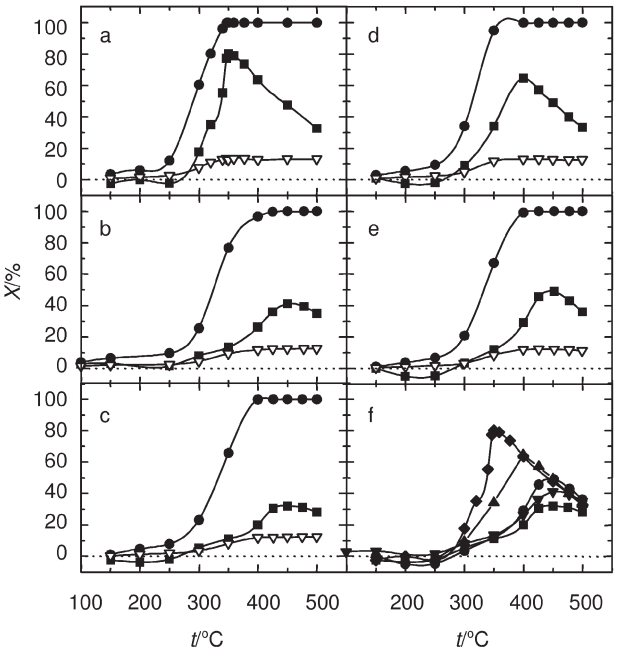

Fig. 2. Conversion of NO (■), C_3H_6 (●), and O_2 (▽) as a function of temperature in the presence of: *a*) ID, *b*) AD, *c*) CAC, *d*) CID, *e*) CAD catalysts. Comparison of NO conversion for ◆ ID, ▼ AD, ■ CAC, ▲ CID, and ● CAD catalysts (*f*).

lic catalysts, dispersion was not affected by the Ru content. The dispersion of bimetallic catalysts appeared to be a function of Ru-Pt interaction magnitude and/or the metal content, especially of Ru content. Similar dispersion of metal particles, around 30 %, was observed for CAC and CAD catalysts, meanwhile, in the case of co-impregnated catalyst higher Ru content led to lower metal dispersion of about 18 %.

In general, moderate metal dispersion was observed for all the catalysts prepared, presenting an appreciable level of interaction between the metal particles and the support.

Catalyst Activity and Selectivity

The activity, conversion *vs.* temperature, curves of NO, C_3H_6, and O_2 for each catalyst are shown in Fig. 2. Comparison of NO conversion *vs.* temperature for the five evaluated catalysts is shown in Fig. 2*f*.

The highest NO conversion of about 80 % was observed when using monometallic catalyst prepared by impregnation. From bimetallic catalysts, that prepared by impregnation-drying procedure showed the highest NO conversion at given conditions. Moreover, the catalysts of I series were the most active as the maximum NO conversion was observed at the lowest reaction temperatures, t_{max}, 50—100 °C lower than the temperature, at which the maximum NO conversion was reached in the presence of A series catalysts. Further incerease of the reaction temperature resulted in the decrease of NO conversion as the oxidation of NO to NO_2 is equilibrium-limited reaction. Equilibrium as a function of temperature was calculated from tabulated data of specific heat capacity variation with temperature, standard formation enthalpy, and standard formation free energy [29]. Obtained values were adjusted to the equation

$$\Delta_r G^o = -57.441 + 0.0758\,T \qquad (4)$$

where the calculated value of $\Delta_r G^o$ is given in kJ mol^{-1}.

When comparing the monometallic AD and ID catalysts, their activity variation should be attributed to the different preparation method and the final metal loading. ID catalyst contained twice as much Ru as AD catalyst. In the case of bimetallic catalysts, the catalytic activity is related to the actual metal content and to the interaction between Ru and Pt atoms of the catalysts. Activity of bimetallic catalysts decreases following the order CID > CAD > CAC, opposite to the interaction strength between the active metals observed by TPR. Moreover, as active metal loading of CAC and CAD catalysts is similar, the activity difference should be attributed exclusively to the magnitude of the metal-metal interaction incited by the catalyst preparation procedure.

In Fig. 3 the concentration of nitrogen-containing compounds, NO, NO_2, N_2O, N_2, and NH_3 in the stream leaving the reactor is shown. Fig. 4 represents the product distribution of C-containing compounds and water vapour as measured in the reactor exhaust gas for the studied catalysts range. N_2, CO_2, and H_2O content shown in Figs. 3 and 4 was calculated according to eqns (*1*—*3*). Concentrations of investigated species for the temperature at which 50 % propylene conversion is reached, t_{50}, and for the temperature at which the maximum NO conversion was observed, t_{max}, are summarized in Tables 2 and 3, respectively.

The principal product of NO oxidation in the presence of Ru-containing catalysts was nitrogen dioxide, as shown in Fig. 3. On the other hand, the presence of NH_3 and N_2O in the gas mixture leaving the reactor was detected. According to results presented in Fig. 4, the main products of propylene combustion were CO_2 and H_2O, even though a small amount of CO was detected. There was no evidence of carbonaceous depots formation on the catalyst surface after the reaction was finished.

Curiously, NO production instead of consumption was observed at lower reaction temperatures (see Figs. 2 and 3) probably due to the reaction of catalyst-activated N_2 [30]. Moreover, at these conditions the presence of oxidizing (O_2) and reducing (C_3H_6) species enables both oxidation of NO to give NO_2, as well as its reduction to N_2O, N_2, and even NH_3.

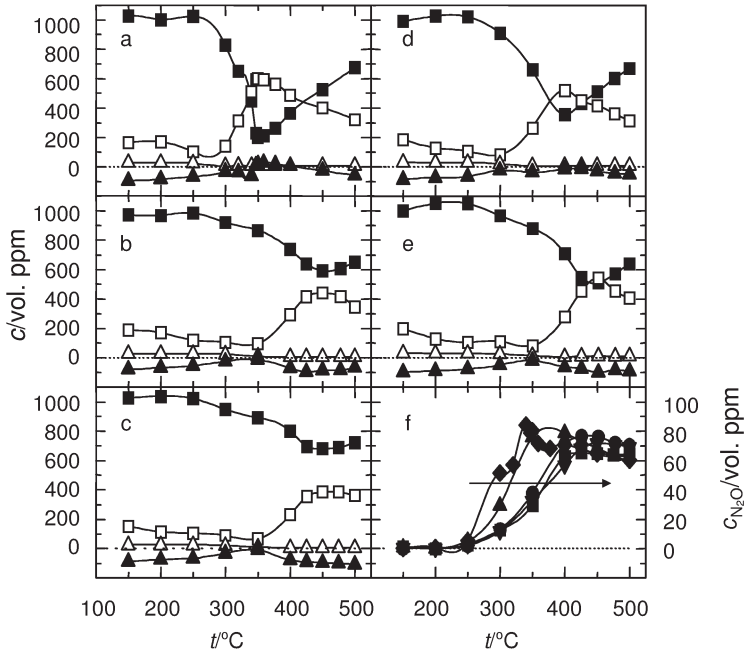

Fig. 3. Concentration of nitrogen-containing species (■ NO, ▲ N_2, □ NO_2, and △ NH_3) in the exhaust gas from the reactor in the presence of: *a*) ID, *b*) AD, *c*) CAC, *d*) CID, and *e*) CAD catalysts. Comparison of N_2O concentration for ◆ ID, ▼ AD, ■ CAC, ▲ CID, and ● CAD catalysts (*f*).

Table 2. Catalyst Activity and Measured Product Distribution in Oxidation of NO (1000 vol. ppm) in the Presence of C_3H_6 (1000 vol. ppm), O_2 (4.5 vol. %), and N_2 (Balance) at t_{50}

Catalyst	t_{50}/°C	c_i/ vol. ppm						φ/vol. %
		NO	N_2O	NO_2	NH_3	C_3H_6	CO	O_2
ID	288	864	45	135	8	500	10	4.21
AD	325	890	22	102	16	500	9	4.19
CAC	332	909	23	76	13	500	13	4.23
CAD	332	910	29	90	17	500	21	4.22
CID	313	840	42	130	15	500	22	4.20

Table 3. Catalyst Activity and Measured Product Distribution in Oxidation of NO (1000 vol. ppm) in the Presence of C_3H_6 (1000 vol. ppm), O_2 (4.5 vol. %), and N_2 (Balance) at t_{max}

Catalyst	t_{max}/°C	c_i/ vol. ppm						φ/vol. %
		NO	N_2O	NO_2	NH_3	C_3H_6	CO	O_2
ID	350	200	80	600	6	1	2	3.94
AD	450	590	72	440	6	2	2	3.94
CAC	450	680	65	385	4	1	1	3.95
CAD	452	511	76	539	10	1	4	3.96
CID	400	355	79	520	6	1	6	3.92

In order to reveal the role of nitrogen in this reaction, He instead of N_2 was used as an inert carrier. During this experiment, the most active, ID, catalyst was heated to a desired temperature ranging from 150 °C to 500 °C using N_2 as the carrier gas. Then, after stabilization, the conversion data were taken and N_2 was replaced with He using the same mass flow controller. The new conversion data for He as carrier gas were taken after stabilization. This procedure was repeated for the following pre-set temperature value. Reactants conversion and product composition variation with temperature for nitrogen and carbon-containing species, measured in the presence of He as carrier gas, are presented in Fig. 5.

Comparing Figs. 5*a* and 2*a* one can conclude that the presence of an inert gas, He, has positive influence on NO as well as propylene conversion at temperatures below 350 °C. Different result was observed

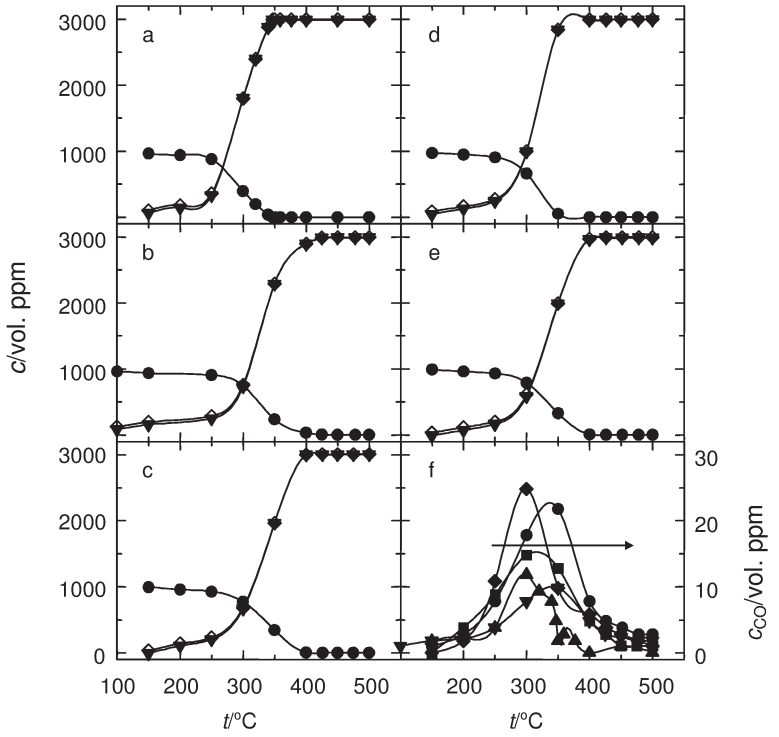

Fig. 4. Concentration of carbon-containing compounds (● C_3H_6 and ◇ CO_2) and H_2O (▼) in the exhaust gas from the reactor in the presence of: *a*) ID, *b*) AD, *c*) CAC, *d*) CID, *e*) CAD catalysts. Comparison of CO concentration for ◆ ID, ▼ AD, ■ CAC, ▲ CID, and ● CAD catalysts (*f*).

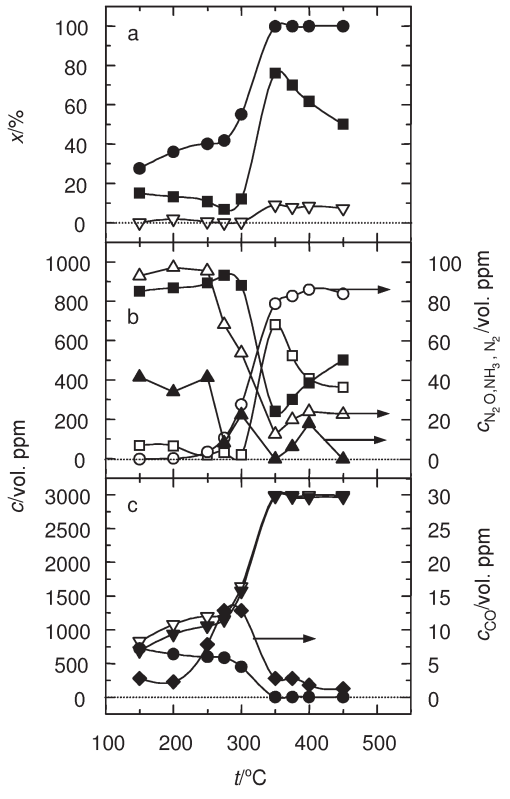

Fig. 5. Conversion of NO (■) over ID catalyst in the presence of C_3H_6 (●) and O_2 (▽) with He as a carrier gas (*a*); the product distribution of nitrogen-containing species (■ NO, ○ N_2O, ▲ N_2, □ NO_2, and △ NH_3) (*b*); and the product distribution of carbon-containing species (● C_3H_6, ◆ CO, and ▽ CO_2) and H_2O (▼) (*c*).

for oxygen consumption. Up to the temperature at which propylene starts burning, in the presence of He, the O_2 conversion never reached 2 %. On the other hand, when nitrogen as the carrier gas was used, the oxygen conversion about 5 % was observed; in spite of being propylene consumption lower (Fig. 4*a*). At higher temperatures, the conversion curves measured for both carrier gases were similar.

Relatively complex is the product distribution obtained at temperatures below 275 ℃ in the presence of He and N_2. According to the results depicted in Figs. 5*b* and 5*c*, NO acted as an oxidizer giving rise to products of total propylene combustion, being reduced itself primarily to ammonia and N_2. When nitrogen was used as a carrier gas (Fig. 3*a*), calculated amount of N_2 was negative suggesting that nitrogen was consumed. Moreover, the amount of NO_2 formed at these conditions in the presence of N_2 was twice the NO_2 content observed when He as the carrier gas was used (Figs. 3*a* and 5*b*, respectively).

Therefore, one may speculate that the relative abundance of the various nitrogen-containing species is ruled by a complex chemical and adsorption equilibrium. Preliminary experiment with a simplified reaction mixture, initially not containing NO, was carried out at the same conditions. In the gas stream leaving the reactor, the measured NO content never exceeded 5 vol. ppm, a value very close to the detector accuracy limit.

The catalyst oxidation capacity towards NO and propylene was found directly related to the ruthenium content, as represented by the t_{50} value in Table 2. ID

was the most active catalyst, giving the highest NO_2 and N_2O yield whilst the lowest CO and NH_3 amount was formed. Its bimetallic analogue, CID, exhibited similar oxidation ability, but the presence of unalloyed Pt resulted in the highest CO amount produced comparing to all studied catalysts. Similar tendency was observed in the case of co-adsorbed catalysts. Again the Ru-Pt interaction reduces the oxidative potential of ruthenium, giving lower NO_2 yield.

In general, at a temperature corresponding to the maximum of NO conversion, t_{max}, complete C_3H_6 conversion occurred (see Table 3). The maximum of CO concentration, not exceeding 25 vol. ppm, was observed for all catalysts at about 300 °C, roughly coinciding with the 50 % propylene conversion (see Tables 2 and 3). On the other hand, CO formation depended on the presence of platinum, as the CO concentration observed when bimetallic catalysts were used exceeded the values measured for the corresponding monometallic catalysts. Furthermore, when catalysts containing both active metals were used, the ability to form CO was proportional to the metal-metal interaction strength. Therefore, the higher was the segregation of ruthenium and platinum phases, the higher was the quantity of carbon monoxide formed.

Acknowledgements. The authors acknowledge the Universidad del País Vasco/EHU for the financial support (UPV 069.310-G40/98) to this research and for a FPI Grant to one of the authors (A. M. S. S.).

SYMBOLS

c	concentration	vol. ppm
D	dispersion	%
T	temperature	K
t	temperature	°C
t_{50}	temperature at which the C_3H_6 conversion reaches 50 %	°C
t_{max}	temperature at which the maximum NO conversion is reached	°C
$\Delta_r G^o$	standard reaction Gibbs energy	kJ mol^{-1}
V_c	cumulative chemisorbed volume of hydrogen	μmol g^{-1}
X	conversion	%
φ	volume fraction	vol. %

REFERENCES

1. Klusom, P. and Cerveny, L., *Appl. Catal., A 128*, 13 (1995).
2. Betancourt, P., Rives, A., Hubaut, R., Scott, C. E., and Goldwasser, J., *Appl. Catal., A 170*, 307 (1998).
3. Berndt, H. and Müller, U., *Appl. Catal., A 180*, 63 (1999).
4. Christoforou, S. C., Efthimiadis, E. A., and Vasalos, I. A., *Ind. Eng. Chem. Res. 41*, 2090 (2002).
5. González-Velasco, J. R., Gutiérrez-Ortiz, M. A., González-Marcos, J. A., Pranda, P., and Steltenpohl, P., *J. Catal. 187*, 24 (1999).
6. Bell, W. E. and Tagami, M., *J. Phys. Chem. 67*, 2432 (1963).
7. Kim, K. S. and Winograd, N., *J. Catal. 35*, 66 (1974).
8. Pinna, F., Scarpa, M., Strukul, G., Guglielminotti, E., Boccuzzi, F., and Manzoli, M., *J. Catal. 192*, 158 (2000).
9. Kobylinski, T. P., Taylor, B. W., and Young, J. E., *SAE Tech. Paper 740250*, 1 (1974).
10. Samsonov, G. V., *The Oxide Handbook*, 26. IFI/Plenum, New York, 1982.
11. Setiabudi, A., Makkee, M., and Moulijn, J. A., *Appl. Catal., B 42*, 35 (2003).
12. Degobert, P., *Automobiles and Pollution.* Editions Technip-SAE, Paris, 1995.
13. Biloen, P. and Sachtler, W. M. H., *Adv. Catal. 30*, 165 (1981).
14. Antolini, E. and Cardellini, F., *J. Alloys Compd. 315*, 118 (2001).
15. Miura, H., Suzuki, T., Ushikubo, Y., Sugiyama, K., Matsuda, T., and Gonzalez, R. D., *J. Catal. 85*, 331 (1984).
16. Sánchez-Sierra, M. C., García-Ruiz, J., Proietti, M. G., and Blasco, J., *J. Mol. Catal. A: Chemical 96*, 65 (1995).
17. Popova, N. M., Antonova, N. A., and Moroz, E. M., *Kinet. Katal. 38*, 692 (1997).
18. Reinikainen, M., Niemelä, M. K., Kakuta, N., and Suhonen, S., *Appl. Catal., A 174*, 61 (1998).
19. Tanabe, K., *Mat. Chem. Phys. 13*, 347 (1985).
20. Chen, F. R., Coudurier, G., Joly, J. F., and Vendrine, J. C., *J. Catal. 143*, 616 (1993).
21. Hino, M. and Arata, K., *Catal. Lett. 30*, 25 (1995).
22. Lu, C.-M. and Lin, Y.-M., *Appl. Catal., A 198*, 223 (2000).
23. Masthan, S. J., *Ind. J. Chem. 35A*, 31 (1996).
24. Serrano-Sánchez, A. M., Blas-Suárez, F., Steltenpohl, P., González-Marcos, M. P., González-Marcos, J. A., and González-Velasco, J. R., in *Scientific Bases for the Preparation of Heterogeneous Catalysts.* (Gaigneaux, E., De Vos, D. E., Grange, P., Jacobs, P. A., Martens, J. A., Ruiz, P., and Poncelet, G., Editors.) Studies in Surface Science and Catalysis 143, pp. 555. Elsevier, Amsterdam, 2002.
25. Brunelle, J. P., in *Preparation of Catalysts II. Scientific Bases for the Preparation of Heterogeneous Catalysts.* (Delmon, B., Grange, P., Jacobs, P. A., and Poncelet, G., Editors.) Elsevier, Amsterdam, 1979.
26. Goodwin, J. G., *J. Catal. 68*, 227 (1981).
27. Díaz, G., Garin, F., Maire, G., Alerasool, S., and Gonzalez, R. D., *Appl. Catal., A 124*, 33 (1995).
28. Buatier de Mongeot, F., Scherer, M., Gleich, B., Kopatzki, E., and Behm, R. J., *Surf. Sci. 411*, 249 (1998).
29. Reid, R. C., Prausnitz, J. M., and Poling, B. E., *The Properties of Gases & Liquids.* 4th Edition. McGraw-Hill, New York, 1987.
30. Glarborg, P., Jensen, A. D., and Johnsson, J. E., *Prog. Energy Combust. Sci. 29*, 89 (2003).